Structure of liquid GeO_2 from a computer simulation model

Gonzalo Gutiérrez*
Departamento de Física, Universidad de Santiago de Chile, Casilla 307, Santiago 2, Chile

José Rogan†
Departamento de Física, Facultad de Ciencias, Universidad de Chile, Casilla 653, Santiago, Chile
(Received 9 June 2003; published 11 March 2004)

The structural properties of liquid GeO_2 are investigated by means of molecular dynamics simulation using a pairwise potential. The simulations were performed in the microcanonical ensemble on systems with up to 576 particles prepared at 21 different densities, corresponding to pressures from -2 to 30 GPa, and temperatures of 1500 K and 3000 K. The pair correlation function, coordination number, angular distribution, and both the neutron and x-ray static structure factors are obtained and compared with those of liquid silica. The analysis of these results for the system at zero pressure indicates that in the liquid state the short range order is dominated by the presence of slightly distorted $Ge(O_{1/2})_4$ tetrahedra. These tetrahedra are linked to each other mainly through the corners, with a Ge-O-Ge angle of $\approx 130°$, similar to the amorphous phase. Beyond the basic tetrahedron some order persists, but to less extent than in liquid silica. Simulation of systems at higher densities shows a volume collapse in the pressure-volume curve in the range of 4–8 GPa, suggesting the possibility that a liquid-liquid phase transition occurs, as the one observed in the amorphous phase.

DOI: 10.1103/PhysRevE.69.031201 PACS number(s): 61.20.Ja, 61.25.−f, 64.90.+b

I. INTRODUCTION

Germanium dioxide (GeO_2), or germania, is a chemical and structural analog to silica (SiO_2), exhibiting similarities in many structural and physical properties. In crystalline state germania has two phases [1]: One low density phase (4.28 g/cm^3) with a quartz structure (Ge coordinated with four oxygens), and a high density phase (6.25 g/cm^3) with rutile structure (Ge coordinated with six oxygens), which is the stable room temperature and pressure structure. Both germania and silica are good glass forming, their structure consisting in a three-dimensional random network composed of basic tetrahedra [$A(O_{1/2})_4$, A=Si,Ge] linked by their vertices.

Silica is a very important material both in technology and geophysics. Phase transitions of minerals under pressure govern several geophysical properties of the earth, where silicates and aluminosilicates play a key role. For example, a detailed knowledge of the structure of silica in the liquid and amorphous states, and its behavior under large applied pressure, is essential to understand the flow of magma [2]. Although germania has not so many applications as silica, from an experimental point of view it is attractive because it presents many properties of silica, but for less extreme conditions. It is known that both noncrystalline silica and germania under pressure present a structural transition from a tetrahedral [$A(O_{1/2})_4$, A=Si, Ge] to an octahedral [$A(O_{1/3})_6$, A=Si, Ge] network, which implies a large change in density and other important physical properties [3,4]. In silica such transformation occurs around 20 GPa, whereas in germania it takes place between 5–9 GPa [5–7], which is more manageable in actual experiments.

Recently the liquid and amorphous phases of a tetrahedral network have been the object of renewed interest because of the so-called polyamorphism. This phenomenon consists in the occurrence of distinct amorphous solid forms of materials and has been observed in tetrahedral systems such as Si, Ge,C,SiO_2,GeO_2 as well as H_2O and Al_2O_3-Y_2O_3 melts, among others [8]. In the case of water and silica, it has been proposed that the polyamorphism of the amorphous solid may be due to a trend towards a liquid-liquid phase separation [9–11] and recent simulations seem to confirm this hypothesis [12–14]. In order to make a theoretical study of this phenomenon, it is necessary to have a reliable model of the liquid as well as a complete characterization of it, both from the structural and dynamic point of view. However, whereas for liquid silica there are several experimental and theoretical studies [15], liquid germania has only been investigated very recently [16].

This contribution presents a computer simulation study on the structural properties of liquid germania. We use molecular dynamics (MD) simulation, which has been proven to be very useful in dealing with the kind of system at hand [17], provided a good interatomic potential is available. This paper is organized as follows: in Sec. II we describe the MD simulation and the preparation of the liquid state. Results for the atomic correlations and diffraction patterns are presented in Sec. III. A discussion of our findings and the conclusions we draw are presented in Sec. IV.

II. COMPUTATIONAL PROCEDURE

Classical molecular dynamic simulations were performed in the microcanonical ensemble (NVE), for a cubic box containing 576 atoms (192 Ge+384 O). We prepare systems at 21 different densities, ranging from 3.0 g/cm^3 to 6.5 g/cm^3

*Electronic address: ggutierr@lauca.usach.cl; URL:http://fisica.usach.cl/~ggutierr

†Electronic address: jrogan@macul.ciencias.uchile.cl; URL: http://macul.ciencias.uchile.cl/ jrogan

TABLE I. Potential parameters.

	A_{ij} (kJ Å^{-6} mol^{-1})	B_{ij} (kJ mol^{-1})	C_{ij} (Å^{-1})
Ge-O	2.2833×10^{4}	$2.006\,96\times10^{7}$	6.129 33
O-O	1.2648×10^{4}	$7.422\,95\times10^{5}$	3.285 11

approximately, which were run at energies corresponding to temperatures T of 3000 K and 1500 K.

A very important issue in MD is the choice of the interatomic potential. Several interatomic potentials have been proposed for covalent materials, most of them incorporating two- and three-body terms, including the ones by Stillinger and Weber [18], Feuston and Garofalini [19], and Vashishta *et al.* [20]. In general, the angle-dependent three-body term is included to properly describe the directional bonds present in covalent materials. However, a breakthrough in the development of a potential including only two-body terms was reported some time ago by Tsuneyuki *et al.* [21] and by van Beest *et al.* [22]. These authors proposed a potential composed by three terms (Coulomb, van der Waals, and repulsion interactions), but the novelty was that the parameters were derived by fitting the model to the potential energy surface of a SiO_4^{-4} cluster, obtained by *ab initio* calculations. This way, they could describe, via a pair potential, the delicate balance of interactions that allows to represent phases with different coordination numbers such as quartz and stishovite. These potentials have also been successfully used to model the silica amorphous-amorphous transition [11], where Si atom changes from coordination 4 at low density to coordination 6 at high density. Thus, it has been demonstrated in practice that this kind of pair potentials are able to reproduce a number of experimental properties, including structural transformations.

To the best of our knowledge, in the literature force fields for liquid germania cannot be found. But, for crystalline germania two model potentials, consisting of pairwise contributions, have been put forward; one by Tsuchiya *et al.* [23] and the other by Oeffner and Elliott [24]. After extensive testing and comparative studies between both potentials [25] we adopted the potential of Oeffner and Elliott [24]. This potential reproduces well both structural and dynamical properties of the two most common crystalline phases of germania, quartz (coordination 4), and rutile (coordination 6). The potential consists of three terms, and has the form

$$V(r_{ij}) = \frac{q_i q_j}{r_{ij}} - \frac{A_{ij}}{r_{ij}^6} + B_{ij}\exp(-C_{ij}r_{ij}), \qquad (1)$$

which represent Coulomb, van der Waals, and repulsion energies, respectively. Here r_{ij} is the interatomic distance between atoms i and j and the effective charges q_i are $q_{\mathrm{Ge}} = 1.5$ and $q_{\mathrm{O}} = -0.75$. The van der Waals coefficients A_{ij}, the softness parameter B_{ij}, and the repulsive radius C_{ij} are the energy parameters, which we displayed in Table I. Notice that this potential only incorporates the interaction between Ge-O and O-O atoms. In the simulations, the long range Coulomb interactions are calculated with the Ewald summation technique and the equations of motion are integrated with a modification of the Beeman algorithm, as is implemented in MOLDY [26], using a time step $\Delta t = 1\times10^{-15}$ s.

The 21 systems were generated starting from a cubic lattice which corresponds to an artificial cristobalite structure with a density of 2.898 g/cm^3. This initial low density system was heated to 5000 K and thermalized for a long time (over 50 000 time steps) to avoid the effects of the initial state on the system. Then the sample was cooled down to 3000 K by scaling velocities at a rate of 0.1 K/Δt and thermalized for 50 000 time steps. With this well equilibrated GeO_2 liquid at 3000 K we prepared 21 systems, reducing simultaneously the lengths of the MD cell and rescaling the positions of all atoms. After this the systems were run for 50 000 time steps and the properties were calculated by taking the average of the last uncorrelated configurations. Finally, using the same cooling schedule, the 21 systems at 1500 K were also obtained.

Notice that these temperatures are well above the glass transition temperature of germania, $T_g \approx 800$ K, and also above its melting temperature $T_m = 1378$ K. In the case of silica these values are $T_g \approx 1500$ K and $T_m = 1995$ K.

III. RESULTS

An overview of the simulations we performed is given in Figs. 1(a) and 1(b), displaying the pressure-volume relation for two different temperatures $T = 3000$ K and $T = 1500$ K, respectively. Note that whereas the high temperature curve exhibits the characteristic shape of a liquid equation of state, at the temperature of 1500 K it presents jumps in the region between 4 and 8 GPa [Fig. 1(b)]. This volume collapse is a fingerprint of a structural transformation associated with a change in the Ge atomic coordination number, from four nearest-neighbors (NN) oxygen atoms at low density (low pressure) to six NN oxygen atoms at high density (high pressure), as it will be discussed in Sec. III C. This structural transformation is well documented for the amorphous case [5], but not so for the liquid state. However, it is known that substances structurally similar to water, such as liquid Si, Ge, SiO_2, and GeO_2, have the potential to exhibit liquid-liquid phase transition [27].

In the following we present the results we obtained for the structural properties of two systems at temperatures of 3000 K and 1500 K, respectively. The density of both is 3.65 g/cm^3, which corresponds approximately to zero pressure. Atomic correlations have been investigated by means of the pair-distribution function, coordination number, and angular distribution. We also present the calculated static scattering structure factors, both for neutrons, $S_N(q)$, and x rays, $S_X(q)$, for these two systems.

A. Atomic correlations

In Figs. 2(a) and 2(b) we display the total and partial pair-distribution functions for 3000 K and 1500 K, respectively. The partial pair-distribution function $g_{\alpha\beta}(r)$ in a binary system is defined in such a way that, sitting on an atom of species α, the probability of finding an atom of the spe-

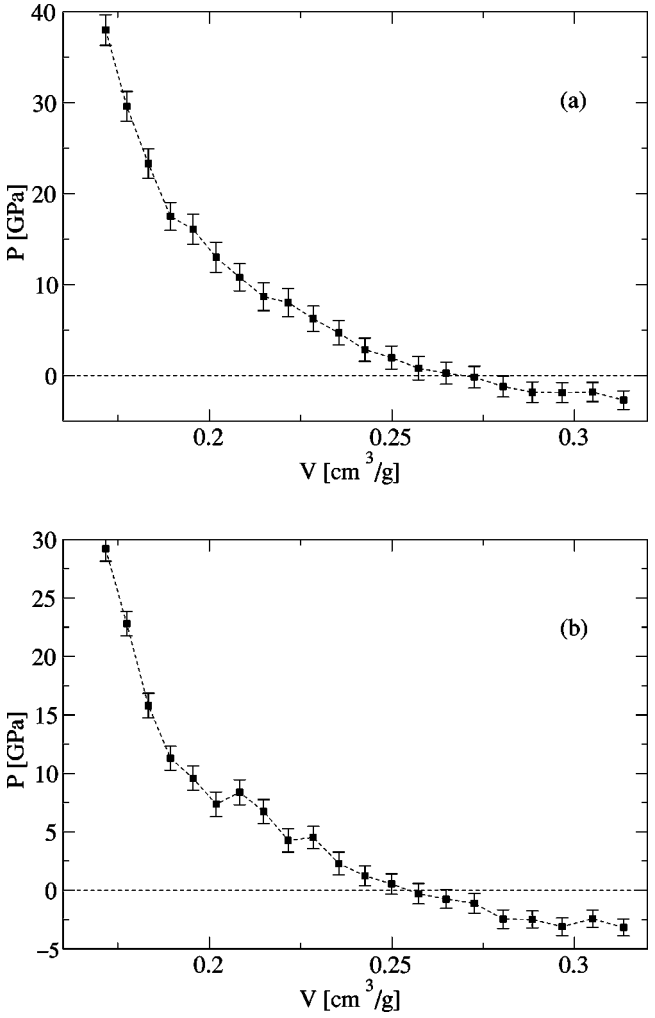

FIG. 1. Equation of state P vs V at (a) $T=3000$ K and (b) $T=1500$ K.

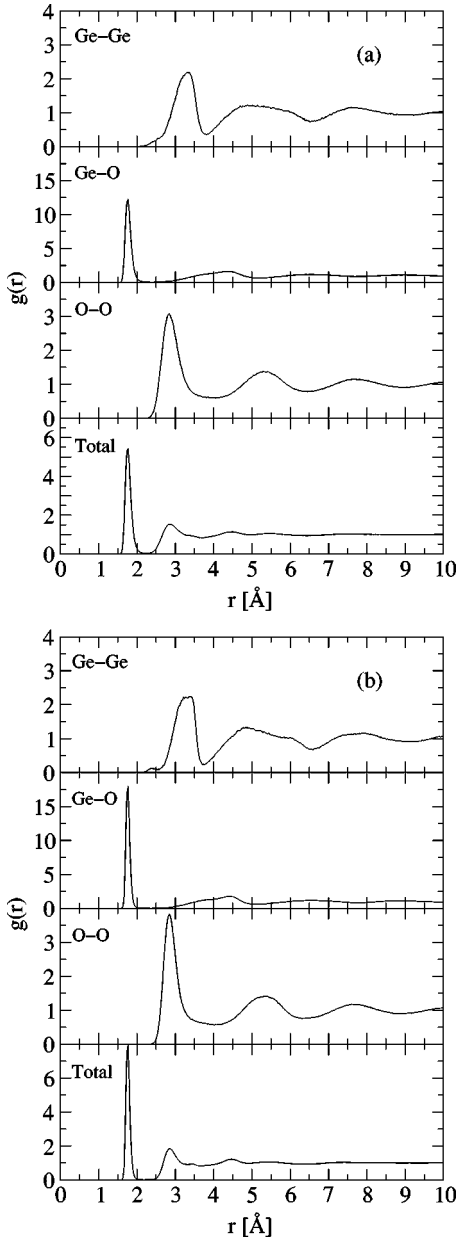

FIG. 2. Pair-distribution function for (a) $T=3000$ K and (b) $T=1500$ K.

cies β inside a spherical shell between r and $r+\Delta r$ is given by $\langle n_{\alpha,\beta}(r,r+\Delta r)\rangle=\rho_\beta 4\pi r^2 g_{\alpha,\beta}(r)\Delta r$, where $\rho_\beta=N_\beta/V$ is the number density of species β, where N_β is the total number of atoms of species β. Comparing Figs. 2(a) and 2(b), we observe that the main changes due to temperature variation are the heights and widths of the peaks: the higher the temperature, the lower and wider the peaks. The same trend is found for the angular distribution, due to the increased disorder induced by higher temperatures. Since the structural properties are quite similar at the temperatures considered here we will limit our attention to the results at $T=1500$ K.

From the position of the first peak of the partial pair-distribution function shown in Fig. 2(b) we find that the Ge-O bond length is 1.7 Å and that the full width at half maximum is 0.15 Å. The NN distances for O-O and Ge-Ge are 2.85 Å and 3.3 Å and the corresponding full width at half maximum are 0.3 Å and 0.5 Å, respectively. In the case of silica, the values of these three NN distances are smaller.

The average coordination number $n_{\alpha\beta}$ is obtained by integration around the first peak of the pair-distribution function, $n_{\alpha\beta}(R)=4\pi\rho_\beta\int_0^R g_{\alpha\beta}(r)r^2dr$, where the cutoff R is usually chosen as the position of the minimum after the first peak of $g_{\alpha\beta}(r)$. Within the cutoff distance $R_{\text{Ge-Ge}}=3.7$, $R_{\text{Ge-O}}=2.2$, and $R_{\text{O-O}}=3.4$ Å, the average nearest-neighbor coordination number of Ge was found to be 4.03 and of O to be 2.01. These values are in agreement with the $8-n$ rule, such as in the case of silica. On the other hand, the Ge atom on the average is surrounded by 4.31 Ge atoms, while the O atom is surrounded by 8.37 O atoms. For silica, the Si atom on the average is surrounded by four Si atoms, but in contrast to germania, the O atom is surrounded by only six O atoms.

The distribution of the coordination numbers for $T=1500$ K is presented in Fig. 3. These histograms are similar to the 3000 K ones. We notice that the Ge-O and O-Ge coordinations have a sharp peak at 4 and 2. However, the

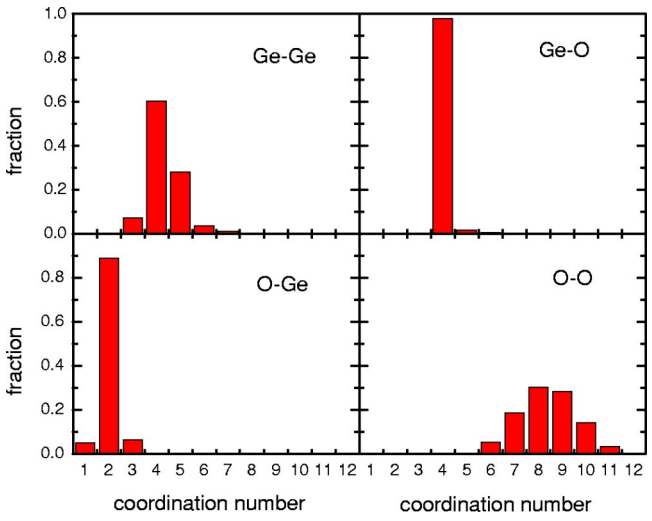

FIG. 3. Histogram of the distribution of Ge and O nearest neighbors at $T=1500$ K.

Ge-Ge and the O-O distributions are broader, because we are counting atoms which belong to the second neighbor shell.

Three-body correlations can be estimated by means of the bond-angle distribution, which provides additional information about the local structural units and their connectivity. Figures 4(a) and 4(b) display the angular distribution for $T=3000$ K and $T=1500$ K, respectively. As in the case of $g(r)$, the only noticeable difference between the $T=3000$ K and $T=1500$ K results is that at 1500 K the peaks are sharper and higher than at 3000 K.

Let us now analyze Fig. 4(b) in detail. The angle O-Ge-O has a peak at 109°, the angle O-O-O has a principal peak centered at 60°, and the angle Ge-O-O has a main peak at 35°. Combining this data with the interatomic distances and coordination numbers already obtained, we conclude that most of Ge and O atoms form a slightly distorted tetrahedron. This is the basic building block of the network, similar to the case of silica. The angle Ge-O-Ge tells us how these tetrahedra are linked to each other. It presents two peaks, a sharp one at 90°, and a higher and broader one at 130°. According to these values, we conclude that the great majority of the tetrahedra are linked through their vertices with an angle around 130°, but also a small percentage is linked by their edges. Notice that in amorphous germania the angle Ge-O-Ge is 133°, less than the amorphous silica angle of 144°, a trend that is repeated in the liquid state case [28]. Interestingly, the smaller Ge-O-Ge angle in germania relative to silica means that germania has a more compacted packing of its basic $Ge(O_{1/2})_4$ units, a fact that is reflected in the O-O coordination numbers, 8 for germania in contrast to 6 for silica.

B. Diffraction pattern

Now we present the MD results for the scattering static structure factor, both for neutrons and x rays, as well as the partial scattering static structure factors. We calculate them in order to analyze these results in relation to liquid silica, and for future comparison with experiments.

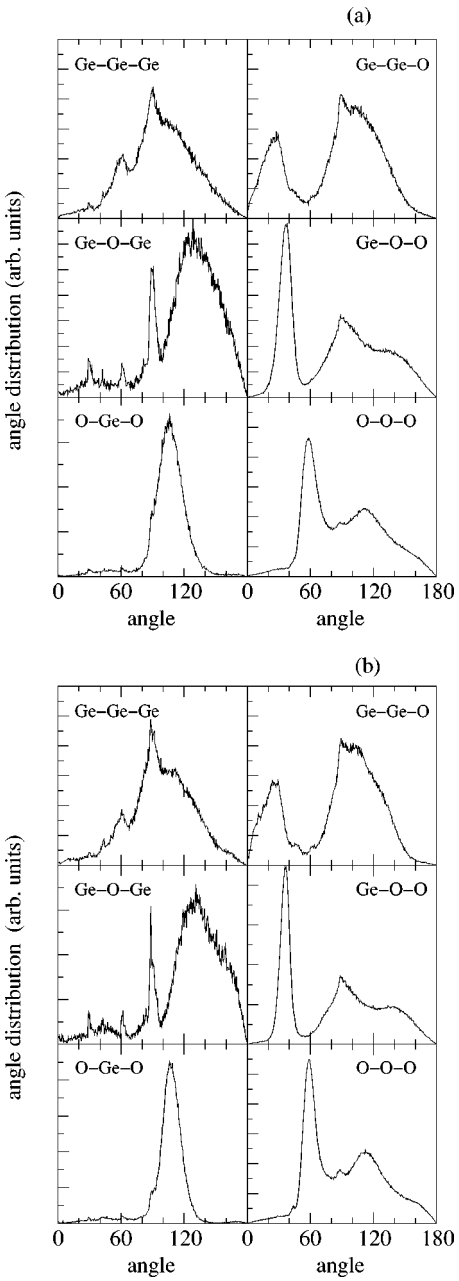

FIG. 4. Angular distributions for (a) $T=3000$ K and (b) $T=1500$ K.

Partial static structure factors are calculated using the Fourier transform of the corresponding partial pair-distribution function, by means of

$$S_{\alpha\beta}(q)=\delta_{\alpha\beta}+4\pi\rho(c_\alpha c_\beta)^{1/2} \times \int_0^R r^2[g_{\alpha\beta}(r)-1]\frac{\sin(qr)}{qr}\frac{\sin(\pi r/R)}{\pi r/R}dr, \tag{2}$$

where $c_{\alpha(\beta)}=N_{\alpha(\beta)}/N$ is the concentration of the $\alpha(\beta)$ species. The window function $\sin(\pi r/R)/\pi r/R$ has been introduced to reduce the termination effects resulting from the

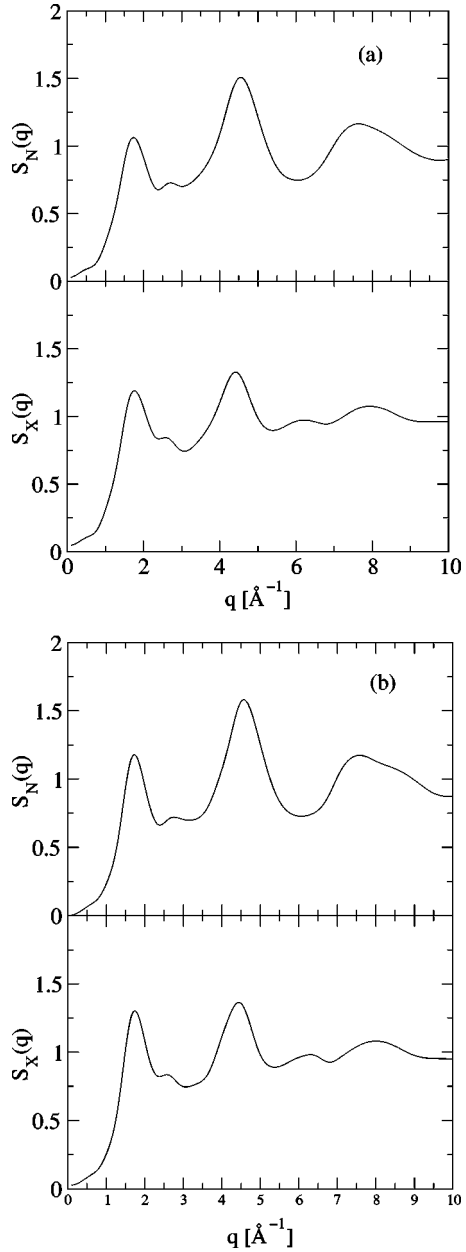

FIG. 5. Neutron and x-ray structure factors at (a) $T=3000$ K and (b) $T=1500$ K.

finite upper limit [29]. The cutoff length R is chosen as one-half the size of the simulation box.

The neutron-scattering static structure factor can be obtained from the partial static structure factors by weighting them with the coherent neutron-scattering lengths

$$S_N(q)=\frac{\sum_{\alpha\beta} b_\alpha b_\beta (c_\alpha c_\beta)^{1/2}[S_{\alpha\beta}(q)-\delta_{\alpha\beta}+(c_\alpha c_\beta)^{1/2}]}{\left(\sum_\alpha b_\alpha c_\alpha\right)^2}, \tag{3}$$

where b_α denotes the coherent neutron-scattering length of species α. We use $b_{\mathrm{Ge}}=0.8193\times10^{-4}$ Å and $b_{\mathrm{O}}=0.5805\times10^{-4}$ Å [30].

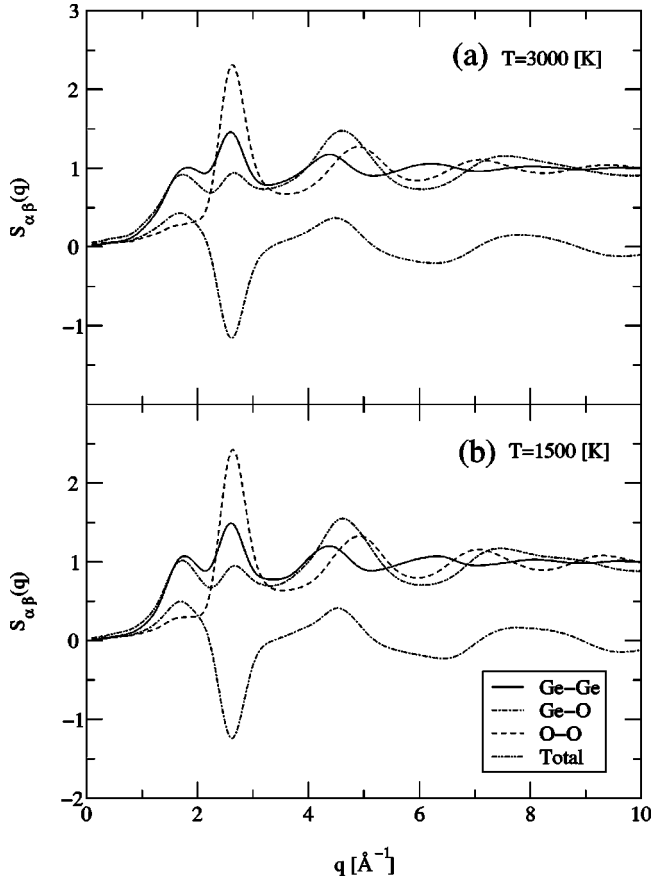

FIG. 6. Partial structure factors at (a) $T=3000$ K and (b) $T=1500$ K.

In a similar way, the x-ray diffraction factor is calculated by means of

$$S_X(q)=\frac{\sum_{\alpha\beta} f_\alpha(q) f_\beta(q)(c_\alpha c_\beta)^{1/2} S_{\alpha\beta}(q)}{\sum_\alpha f_\alpha^2(q) c_\alpha}, \tag{4}$$

where $f_\alpha(q)$ is the q-dependent x-ray form factor, given by

$$f_\alpha(q)=\sum_{i=1}^{4} a_{\alpha,i}\exp[-b_{\alpha,i}(q/4\pi)^2]+c_\alpha. \tag{5}$$

The parameters $a_{\alpha,i}$, $b_{\alpha,i}$, and c_α are taken from Ref. [31] for aluminum and Ref. [32] for oxygen.

Figure 5(a) shows the MD results for the neutron static structure factor $S_N(q)$ and the x-ray structure factor $S_X(q)$, for the sample at $T=3000$ K, and Fig. 5(b) displays the results for $T=1500$ K. All figures show the characteristic peaks of a liquid. The main features are that the first peak occurs at approximately $q=1.7$ Å^{-1}, followed by a small peak at 2.6 Å^{-1}, and finally a third peak at 4.5 Å^{-1}. In analogy to the amorphous case, we can associate the third peak with the short range order, expressed in real space by the $Ge(O_{1/2})_4$ tetrahedron. The peaks at lower q would be responsible for real space correlations beyond ≈4 Å. Com-

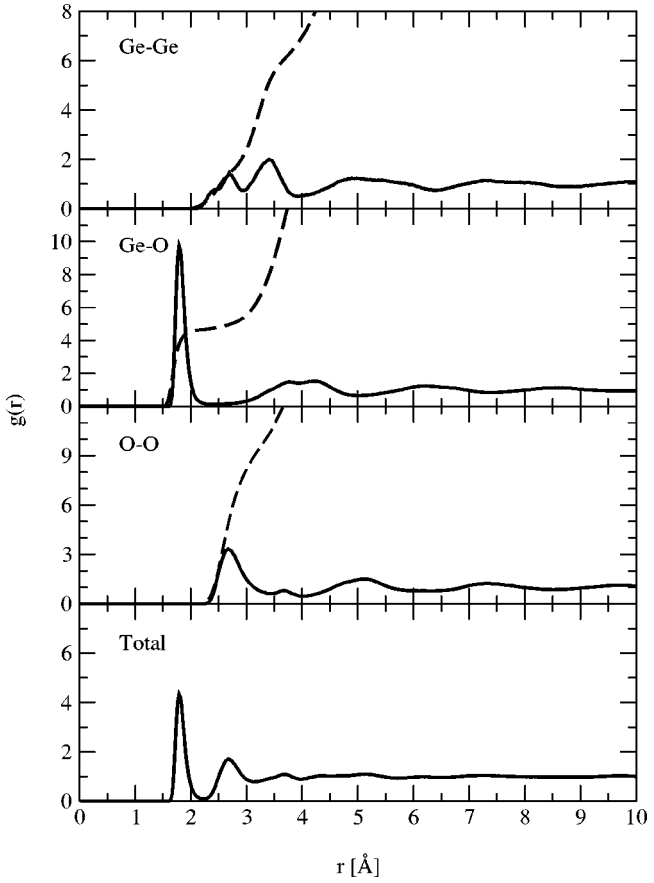

FIG. 7. Pair-distribution function (full line) and coordination numbers (dash line) at $T=1500$ K and density of 5.15 g/cm^3.

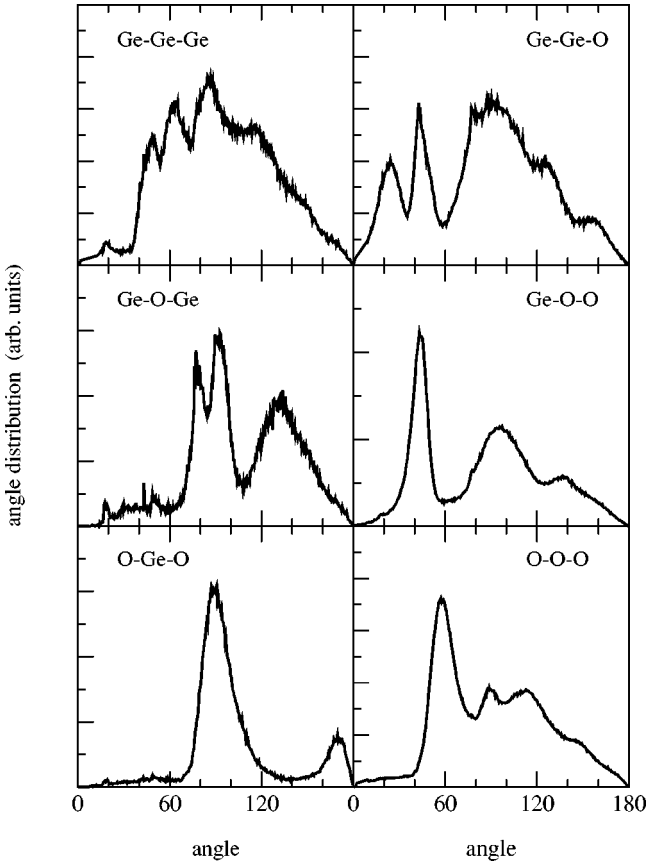

FIG. 8. Angular distribution function at $T=1500$ K and density of 5.15 g/cm^3.

paring to amorphous germania [33], we can see that the two latter peaks coincide, but that the first peak is located at a smaller q value, 1.54 Å^{-1}, in the amorphous case.

The origin of the peaks of $S_N(q)$ and $S_X(q)$ can be inferred from the partial static structure factor $S_{\alpha\beta}(q)$ calculated from MD trajectories by means of Eq. (2). The results are shown in Fig. 6 for $T=3000$ K and for $T=1500$ K. These results indicate that the first peak of the total static structure factor $S(q)$ [as well as in the $S_N(q)$ and $S_X(q)$] is mainly due to Ge-Ge and Ge-O correlations. The second peak arises from Ge-Ge and O-O correlations, including partial cancellation from Ge-O anticorrelations. The third peak is due to all three correlations. Comparing these results to the simulation on liquid silica, we can see that in liquid silica the first peak is sharper than in our case and is due to all three correlations [20].

C. Structural properties at high pressure

At the beginning of this Sec. III we noticed that systems at higher densities show a volume collapse in the pressure-volume curve in the range of 4–8 GPa, suggesting the possibility that a liquid-liquid phase transition occurs, as the one observed in the amorphous phase. Further insight into such transformation can be obtained by analyzing the structural properties of a system at high density (high pressure). We choose a system with a density of 5.15 g/cm^3, corresponding to a pressure of $\approx$11 GPa [35]. The pair-distribution function and coordination numbers are presented in Fig. 7, and the angular distribution in Fig. 8.

From the full curves of Fig. 7 we can see that for this system at high density the Ge-Ge first peak splits into two peaks, with the first of these peaks located at 2.7 Å, and the second at 3.4 Å. In a similar way, the O-O NN distance decreases from 2.85 Å at normal density to 2.65 Å at the high density. The inverse trend is found for the Ge-O bond length which increases with the density from 1.7 to 1.8 Å. At distances beyond the nearest neighbors, the pair-distribution function presents more structure at high density compared to normal density. Useful supplementary information can be obtained from the average coordination numbers $n_{\alpha\beta}(R)$, which is represented in Fig. 7 by a dashed line. Depending on the cutoff R, the Ge-Ge coordination numbers is 2.5 up to the first peak ($R=3$ Å) and 6.4 at $R=3.7$. The Ge-O and the O-Ge coordination numbers are 5.2 and 3, respectively, at $R=2.5$. Finally, the O-O coordination number is 11.3 at $R=3.5$ Å. Thus, we have a transition from a system of low coordination numbers at normal density to one with high coordination numbers at high density. All these facts constitute an indication that a major structural transformation does take place, from an open to a closed packedlike structure.

We can gain further insight into the nature of the high density phase analyzing the angular distribution presented in

TABLE II. Density, bond length, bond angle, Ge-O-Ge angle, and bulk modulus of germania.

Phase	Density (g/cm^3)	Bond length (Å)	Ge-O Coordination number	O-Ge-O Angle	Ge-O-Ge Angle	Bulk modulus (GPa)
Quartz[a]	4.28	1.737	4	113,106	130	39.2
		1.741		110,107	129	
Rutile[b]	6.25	1.871	6	80.2	130.1	258
		1.903				
Amorphous[c]	3.7 ± 0.1	Ge-O ≈1.73	4	109	133	30 ± 2
		O-O ≈2.83		(104–115)	$\sigma\approx8.3$	
		Ge-Ge ≈3.16				
Liquids	3.65	Ge-O ≈1.7	4	109	130	
(This work)		O-O ≈2.85			$\sigma\approx30$	
		Ge-Ge ≈3.3				

[a]References [23,24,28].
[b]References [23,24,28].
[c]Reference [34].

Fig. 8. The three angles that reflect the structure of the basic building block of the network are the O-Ge-O, Ge-O-O, and O-O-O, angles. We can see that the main peak at O-Ge-O angle changes from 109° at normal density to 90° at high density, and also a small peak does appear at $\approx170°$. The angle Ge-O-O shifts one of its peaks from 35° at normal density to 45° at high density, while the other two peaks remain fixed. Finally, the peaks of the angle O-O-O remain the same, except that the height of the peak at 90° increases. It is not difficult to infer that these data are consistent with an octahedral arrangement, with the Ge atom at the center and the oxygen atoms in the vertex. Combining this information with the interatomic distances and the coordination numbers, we conclude that at high density the elementary unit of the system is mainly a slightly distorted octahedron. The nearest-neighbor connectivity of these elementary units is described by the Ge-O-Ge angular distribution. Comparing it with the distribution at low density we see that the small peak at 90° increases, and the large peak at 130° decreases, changing the system from a mostly corner-sharing tetrahedral network at low density to a network which mostly contains octahedra as basic units, linked to each other by the corners, as well as by the edges and/or faces.

IV. CONCLUDING REMARKS

Table II presents a summary of our findings for liquid germania together with experimental data of GeO_2, both in the crystalline and the amorphous state, all of them at room pressure. The data of the liquid state correspond to a temperature of 1500 K. At room temperature and pressure the stable crystalline phase is rutile, with a Ge-O coordination number of 6. However, in the liquid state, germania suffers a large expansion, lowering its density more than 40%, resulting in a Ge-O coordination number of 4. This behavior sharply contrasts with the silica case, where the stable crystalline phase, quartz, has the same Si-O coordination number 4 as its liquid phase.

The MD results for systems at 21 different densities at a temperature of 1500 K show a volume collapse in the pressure versus volume plot, in the range of 4–8 GPa. The analysis of a system at the density of 5.15 g/cm^3 reveals that a major structural transformation takes place, from an open structure at low density to a closed packedlike structure at high density. These facts are indicative that a liquid-liquid phase transition is very likely to occur, as is the case for the amorphous phase.

According to our results we conclude that in liquid germania there exists a well-defined short range order, dominated by a slightly distorted tetrahedron. In the network most of these tetrahedra are linked to each other by corners, at an angle Ge-O-Ge of $\approx130°$. Then, at few angstroms beyond this basic tetrahedron, there still persists some degree of order. This kind of intermediate range order is reflected in the two first peaks of the static structure factor and in the real space correlations of the radial distribution and angular distribution functions. From this point of view liquid germania is similar to liquid silica, although in the latter case this kind of intermediate range correlations are much more marked than in the former one. In order to explain this fact it would be useful to perform an electronic structure calculation on both these systems. One can speculate that this difference could be explained by the increased metallicity of germanium relative to silicon, which induces a closed packedlike structure, increasing the number of neighbors and therefore the disorder in the network.

ACKNOWLEDGMENTS

This work was supported by FONDECYT (Chile) under Grant Nos. 1030063 (G.G.), 8990005, and 1030957 (J.R.). G.G. also acknowledges the *Núcleo Materia Condensada-Iniciativa Científica Milenio* ICM. The authors thank M. Kiwi for a critical reading of the manuscript.

[1] D.M. Christie and J.R. Chelikowsky, Phys. Rev. B **62**, 14 703 (2000).
[2] J.L. Yarger *et al.*, Science **270**, 1964 (1995).
[3] S. Sugai and A. Onodera, Phys. Rev. Lett. **77**, 4210 (1996); R.J. Hemley, C. Meade, and H.-K. Mao, *ibid.* **79**, 1420 (1997); J. Swenson, *ibid.* **79**, 1421 (1997).
[4] C.E. Stone *et al.*, J. Non-Cryst. Solids **293-295**, 769 (2001).
[5] J.P. Itie, A. Polian, G. Calas, J. Petiau, A. Fontaine, and H. Tolentino, Phys. Rev. Lett. **63**, 398 (1989).
[6] K.H. Smith, E. Shero, A. Chizmeshya, and G.H. Wolf, J. Chem. Phys. **102**, 6851 (1995).
[7] C.H. Polsky, K.H. Smith, and G.H. Wolf, J. Non-Cryst. Solids **248**, 159 (1999).
[8] P.H. Poole, T. Grande, C.A. Angell, and P.F. McMillan, Science **275**, 322 (1997).
[9] P.H. Poole, F. Sciortino, U. Essmann, and H.E. Stanley, Nature (London) **360**, 324 (1992).
[10] P.H. Poole, M. Hemmati, and C.A. Angell, Phys. Rev. Lett. **79**, 2281 (1997).
[11] D.J. Lacks, Phys. Rev. Lett. **84**, 4629 (2000).
[12] C.J. Roberts, A.Z. Panagiotopoulos, and P.G. Debenedetti, Phys. Rev. Lett. **77**, 4386 (1996).
[13] S. Harrington, R. Zhang, P.H. Poole, F. Sciortino, and H.E. Stanley, Phys. Rev. Lett. **78**, 2409 (1997).
[14] I. Saika-Voivod, F. Sciortino, and P.H. Poole, Phys. Rev. E **63**, 011202 (2000).
[15] See, for example, A. Trave, P. Tangney, S. Scandolo, A. Pasquarello, and R. Car, Phys. Rev. Lett. **89**, 245504 (2002), and references therein.
[16] See, for example, A. Meyer, H. Schober, and J. Neuhaus, Phys. Rev. B **63**, 212202 (2001).
[17] M.P. Allen and D.J. Tildesley, *Computer Simulation of Liquids* (Clarendon Press, Oxford, 1994).
[18] F.H. Stillinger and T.A. Weber, Phys. Rev. B **31**, 5262 (1985).
[19] B. Feuston and S.H. Garofalini, J. Chem. Phys. **89**, 5818 (1988).
[20] P. Vashishta, R.K. Kalia, J.P. Rino, and I. Ebbsjo, Phys. Rev. B **41**, 12 197 (1990).
[21] S. Tsuneyuki, M. Tsukada, H. Aoki, and Y. Matsui, Phys. Rev. Lett. **61**, 869 (1988).
[22] B.W.H. van Beest, G.J. Kramer, and R.A. van Santen, Phys. Rev. Lett. **64**, 1955 (1990).
[23] T. Tsuchiya, T. Yamanaka, and M. Matsui, Phys. Chem. Miner. **25**, 94 (1998).
[24] R.D. Oeffner and S.R. Elliott, Phys. Rev. B **58**, 14 791 (1998).
[25] G. Gutiérrez and J. Rogan (unpublished).
[26] K. Refson, MOLDY, a general-purpose molecular dynamics code. Available free for academic purpose at http://www.earth.ox.ac.uk/~keith/ moldy. html, Release 2.13 1998.
[27] P. G. Debenedetti, *Metastable Liquids: Concepts and Principles* (Princeton University Press, Princeton, NJ, 1998).
[28] R. Hussin, R. Dupree, and D. Holland, J. Non-Cryst. Solids **246**, 159 (1999).
[29] E.A. Lorch, J. Phys. C **2**, 229 (1969).
[30] L. Koester, H. Rauch, M. Herkens, and K. Schrder, Jülich Report No. Jül-1755 1981 (unpublished).
[31] D.T. Cromer and J.T. Waber, in *International Tables for x-Ray Crystallography*, edited by J.A. Ibers and W.C. Hamilton (Kynoch Press, Birmingham, 1974).
[32] M. Tokonami, Acta Crystallogr. **19**, 486 (1965).
[33] D.L. Price, M-L. Saboungi, and A.C. Barnes, Phys. Rev. Lett. **81**, 3207 (1998).
[34] O.B. Tsiok, V.V. Brazhkin, A.G. Lyapin, and L.G. Khvostantsev, Phys. Rev. Lett. **80**, 999 (1998).
[35] Further analysis about this transition will be presented elsewhere.